C-FIELD REPRESENTATION OF COMPLIANCE IN LUMPED-PARAMETER FINITE-MODE REPRESENTATIONS OF CONTINUOUS SYSTEMS WITH MULTIPLE FORCE INPUTS

Layne Clemen
Extensible Energy
San Diego, California, USA. Email:layne@extensibleenergy.com

Donald L. Margolis
Department of Mechanical Engineering and Aerospace Engineering
University of California, Davis, USA. Email:dlmargolis@ucdavis.edu

ABSTRACT

Engineers are constantly working with systems coupled through components that require their distributed dynamic effects are taken into consideration. This paper represents a method to correctly represent the compliance of a lumped-parameter finite-mode representation of a continuous system. To accurately represent the deflections in the system, a residual compliance is required beyond the first n-modal compliances. The equations for the C-field entries of a generic m-force continuous system are derived including the residual compliance. Once the C-field equations are derived, the causality considerations for integrating residual compliances are discussed. Using these results, an example of a simply-supported Bernoulli-Euler beam with two force inputs is developed for the reader and results are shown with and without the correct residual compliance. Additionally, an example of a cart with a mass attached to a flexible beam is presented showing that residual modes will occur when the residual compliance is integrated into larger systems models. This gives the user a powerful tool to integrate modal information into their models that has been shown to increase fidelity in other applications like finite element analysis.

Keywords: Continuous Systems, Modal Analysis, Residual Compliance.

1 INTRODUCTION

Controlled systems, especially position control systems, are always mounted on some sort of structure. In many cases modal information is not required to accurately control the system and meet the design objectives. However, there are situations, such as vehicle and aerospace structures (Margolis 1985, Mukherjee, Siegler, and Thronson 2019) , where the modal information can become critical to meeting objectives and verifying stability. Bond Graphs provide a simple way of including modal information for a structure. As most engineers should know, there are an infinite number of modes in any system but retaining a large number of modes is not practical or required for the types of models and analysis that bond graphs are generally employed for. While this pruning of modes makes sense from a computational point of view, it can have unintended consequence of altering the dynamic response of the analysis to the point that it is no longer appropriate. In order to handle this situation, the user can calculate a residual compliance that represents that compliance associated with the pruned modes. Adding this into the model corrects steady-state deflections and makes residual modes appear in the system due to interaction between structural

ICBGM'2021 Nov 8-10, 2021- San Diego, California USA -

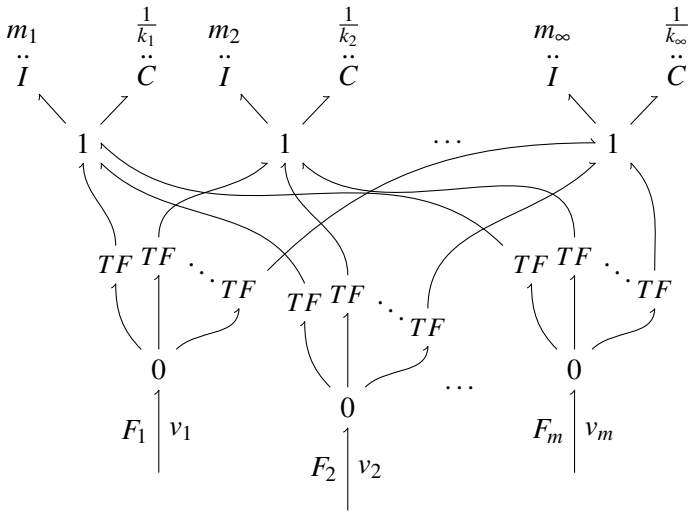

Figure 1: SYSTEM BOND GRAPH

and system components. The reduction in error at higher frequencies by including these residual modes is well known in the structural dynamics community (Blelloch, Dickens, Majed, and Sills 2019) but generally done in Hurty/Craig-Bampton models of large Finite Element Model (FEM) systems. For systems of interest to a bond graph modeler, the residual compliance is a field of size $m \times m$ where m indicates the number of points of interaction between the structural element and other system components. In this paper a general method for calculating the residual compliance field is presented. While it would be great if there were always a closed form solution for steady-state deflections fo a structural element, the required information will most likely come from a FEM simulation. Luckily the analysis lends itself to the information coming from either source. The paper is organized as follows: First, the residual compliance calculations are developed and resented for the general m-input case. Second, causal considerations are analyzed and a closed form solution is presented for a residual compliance field with a mixed-causality assignment. Next, two simple examples are presented for a fixed-fixed Bernoulli-Euler beam and a cart with a flexible mass attached to a vertical beam. Finally, conclusions and future work are discussed.

2 DEVELOPMENT

The bond graph in Fig. 1 represents a fixed continuous system represented by infinite modes with interfaces at m-locations. The modulus of each transformer ($Y_{i,j}$) is the mode shape i at location j or the connection between the i^{th} 0-junction interface and the j^{th} 1-junction that represents mode-j. It should be obvious that as $n \to \infty$, the system will represent the partial differential solution of the continuum center line with infinite modes. The transformer moduli have been omitted from the bond graph for cleanliness. If there system were not fixed, the user would simply include any rigid body modes in the model.

For a veteran bond graph user, it should be obvious that the velocities at each interface will be calculated with the following equation

$$v_i = \sum_{j=1}^{\infty} \frac{Y_{i,j}}{m_j} p_j \tag{1}$$

From this bond graph and Eq (1) it should be easy to see that the displacement at each node (δ_i) can be found by integrating Eq.(1).

$$\delta_i = \int v_i dt = \sum_{j=1}^{\infty} Y_{i,j} q_j \tag{2}$$

Now consider a system where n-modes have been retained. A residual compliance-field must be

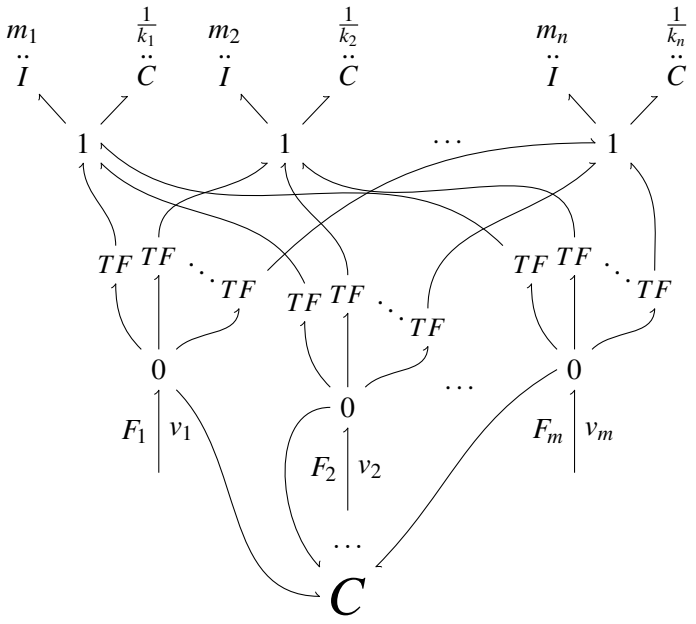

Figure 2: AUGMENTED MODAL SYSTEM BOND GRAPH

calculated and attached to each 0-junction that represents the effort inputs into the system. This will result in an added multi-port as shown in Fig. 3. Adding the residual compliance field results in the augmented bond graph shown in Fig. 2.

The find the constitutive law for the required C-field, start with Eq. (2) at each node.

$$\delta_1 = Y_{11}q_1 + Y_{12}q_2 + \ldots + Y_{1n}q_n \tag{3}$$

$$\delta_2 = Y_{21}q_1 + Y_{22}q_2 + \ldots + Y_{2n}q_n \tag{4}$$

$$\vdots$$

$$\delta_m = Y_{m1}\dot{q}_1 + Y_{m2}\dot{q}_2 + \ldots + Y_{mn}\dot{q}_n \tag{5}$$

Now inserting the constitutive law

$$q_j = C_j\left[Y_{1j}F_2 + Y_{2j}F_2 + \ldots + Y_{mj}F_m\right] \tag{6}$$

where $C_j = 1/k_j$, into Eqs. (3-5) results in the following equation

$$\delta = \mathbf{CF} \tag{7}$$

Where

$$\delta = \begin{bmatrix}\delta_1 & \delta_2 & \vdots & \delta_m\end{bmatrix}^T \tag{8}$$

$$\mathbf{F} = \begin{bmatrix}F_1 & F_2 & \vdots & F_m\end{bmatrix}^T \tag{9}$$

$$\mathbf{C} = \begin{bmatrix} \sum_k Y_{1k}^2 C_k & \sum_k Y_{1k}Y_{2k}C_k & \ldots & \sum_k Y_{1k}Y_{mk}C_k \\ \sum_k Y_{1k}Y_{2k}C_k & \sum_k Y_{2k}^2 C_k & \ldots & \sum_k Y_{2k}Y_{mk}C_k \\ \vdots & & \ddots & \vdots \\ \sum_k Y_{1k}Y_{mk}C_k & \sum_k Y_{2k}Y_{mk}C_k & \ldots & \sum_k Y_{mk}^2 C_k \end{bmatrix} \tag{10}$$

It should be noted to the reader that **C** is a symmetric matrix where the each coefficient can be found with the equation

$$c_{ij} = \sum_{k=1}^{n} Y_{ik}Y_{jk}C_k \tag{11}$$

and

$$c_{ij} = c_{ji} \tag{12}$$

This is as expected due to Maxwell reciprocity in fields (Karnopp, Margolis, and Rosenberg 2012). For some systems, such as a fixed-fixed beam, one can find the steady state displacements as a function of the applied forces that can be equated to the modal displacements that takes the form

$$\begin{bmatrix}\delta_1 \\ \delta_2 \\ \vdots \\ \delta_m\end{bmatrix} = \underbrace{\begin{bmatrix} C_{11} & C_{12} & \ldots & C_{1m} \\ C_{21} & C_{22} & \ldots & C_{2m} \\ \vdots & & \ddots & \vdots \\ C_{m1} & C_{m2} & \ldots & C_{mm}\end{bmatrix}}_{\mathbf{C_{ss}}} \begin{bmatrix}F_1 \\ F_2 \\ \vdots \\ F_m\end{bmatrix} \tag{13}$$

Subtracting Eq. (7) from Eq. (13) results in a residual of the form

$$\delta = \mathbf{C}_r \mathbf{F} \tag{14}$$

Where

$$\mathbf{C}_r = \begin{bmatrix} C_{11} - \sum_k Y_{1k}^2 C_k & C_{12} - \sum_k Y_{1k} Y_{2k} C_k & \dots & c_{r_{1m}} \\ C_{21} - \sum_k Y_{1k} Y_{2k} C_k & C_{22} - \sum_k Y_{2k}^2 C_k & \dots & c_{r_{2m}} \\ \vdots & & \ddots & \vdots \\ c_{r_{m1}} & c_{r_{m2}} & \dots & c_{r_{mm}} \end{bmatrix} \tag{15}$$

and

$$c_{r_{ij}} = C_{ij} - \sum_{k=1}^{n} Y_{ik} Y_{jk} C_k \tag{16}$$

In all reality, an analytical result for $c_{r_{ij}}$ is not realistic and the summation should be found by iterating numerically until the value converges to an acceptable level. This should happen quite quickly. In more complex systems, an analytical solution is not guaranteed and should not be expected. In this case, the modal information will either be found by using an FEA solver or testing and extracting the relevant modal information. If enough modal information is available, the residual compliances must be calculated from the following equation

$$c_{r_{ij}} = \sum_{k=n+1}^{\infty} Y_{ik} Y_{jk} C_k \tag{17}$$

In the case of a system that can move freely, i.e. a free-free beam this will also apply. When higher mode information is not available, one could find the steady-state deflections due to a known force input. In this case the total deflection (δ) will follow Eq. (13). Now the deflection due to the included modes can be found using Eq. (7) and the known force. It is straight forward that the displacement due to the residual compliance is

$$\delta_r = \delta - \mathbf{C}\mathbf{F} = \mathbf{C}_r \mathbf{F} \tag{18}$$

Unfortunately, one needs to simulate the system with m-linearly independent force input vectors. In this case, it is easiest to use a unit input at each point. This results in m-displacement vectors. In the case of unit force inputs the matrix $[\mathbf{F}_1, \mathbf{F}_2, \dots, \mathbf{F}_m] = \mathbf{I}_{m \times m}$ which results in a matrix of displacements $\Delta = [\delta_1, \delta_2, \dots, \delta_m]$ and $\mathbf{C}_r$ can be calculated by

$$\mathbf{C}_r = \Delta - \mathbf{C} \tag{19}$$

In general, the modal information should be available so this approach will not be needed.

2.1 CAUSALITY CONSIDERATIONS

As with all bond graphs, integral causality is not guaranteed in the final form. The C-field representing the residual compliance can easily find itself in derivative or mixed causality leading to additional equation formulation requirements. To that end, the general derivative causality solution method can be applied to the field. First look at a mixed causality C-field.

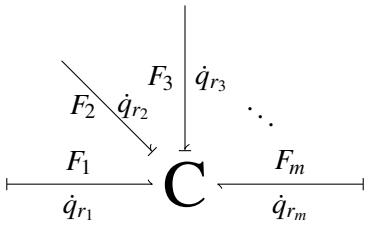

Figure 3: MIXED CAUSALITY C-FIELD

Putting the field into the generic displacement-effort relationship of Eq (14) and rearranging the displacement and forces vectors into input forces ($\mathbf{F_i}$), output forces ($\mathbf{F_o}$), input displacements ($\delta_\mathbf{i}$), and output displacements ($\delta_\mathbf{o}$) results in the following matrix equation.

$$\begin{bmatrix} \mathbf{q_i} \\ \mathbf{q_o} \end{bmatrix} = \begin{bmatrix} \mathbf{C_{io}} & \mathbf{C_{ii}} \\ \mathbf{C_{oo}} & \mathbf{C_{oi}} \end{bmatrix} \begin{bmatrix} \mathbf{F_o} \\ \mathbf{F_i} \end{bmatrix} \tag{20}$$

In this case, the output forces ($\mathbf{F_o}$) are on the causal bonds and output displacements ($\mathbf{q_o}$) are on the acausal bonds. The inputs, $\mathbf{q_i}$ and $\mathbf{F_i}$, are coupled with their corresponding causal assignment. Rearranging Eq. (20) into I/O form results in the following matrix equation

$$\underbrace{\begin{bmatrix} -\mathbf{C_{io}} & \mathbf{0_o} \\ -\mathbf{C_{oo}} & \mathbf{I_o} \end{bmatrix}}_{\mathbf{M}} \begin{bmatrix} \mathbf{F_o} \\ \mathbf{q_o} \end{bmatrix} = \begin{bmatrix} \mathbf{C_{ii}} & -\mathbf{I_i} \\ \mathbf{C_{oi}} & \mathbf{0_i} \end{bmatrix} \begin{bmatrix} \mathbf{F_i} \\ \mathbf{q_i} \end{bmatrix} \tag{21}$$

Using the Schur complement (Petersen, Pedersen, et al. 2008), one can solve for the inverse of $\mathbf{M}$ and find the required I/O relationship to solve the derivative causality loop.

$$\begin{bmatrix} \mathbf{F_o} \\ \mathbf{q_o} \end{bmatrix} = \begin{bmatrix} -\mathbf{C_{io}}^{-1}\mathbf{C_{ii}} & \mathbf{C_{io}}^{-1} \\ \mathbf{C_{oi}} - \mathbf{C_{oo}}\mathbf{C_{io}}^{-1}\mathbf{C_{ii}} & \mathbf{C_{oo}}\mathbf{C_{io}}^{-1} \end{bmatrix} \begin{bmatrix} \mathbf{F_i} \\ \mathbf{q_i} \end{bmatrix} \tag{22}$$

Note: It should be obvious that when the C-field is in complete derivative causality, one simply needs

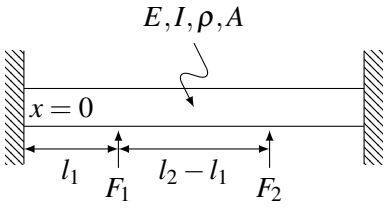

Figure 4: EXAMPLE 1 - FIXED-FIXED BERNOULLI EULER BEAM

to differentiate both sides to find the relationship

$$\dot{\mathbf{q}} = \mathbf{C_r}\dot{\mathbf{F}} \tag{23}$$

where $\mathbf{F}$ *is found from the attached subsystems.*

As can be seen, without the residual compliance, any attached subsystem setting the velocity on one of the nodes would result in derivative causality on one of the modes. The residual compliance acts as a buffer to acausal modal states. However this is not for free. When the effort on an input bond is set by an external subsystem, derivative causality results, begging the question of adding a small mass between the attached subsystem and node of interest to alleviate the derivative causality issue.

3 EXAMPLES

Both of these examples are simple but illustrate the importance of including the residual compliance in dynamic models of continuous systems. In both examples the residual compliance is taken as

$$\mathbf{C_r} = \begin{bmatrix} c_{r_{11}} & c_{r_{12}} \\ c_{r_{21}} & c_{r_{22}} \end{bmatrix} \tag{24}$$

3.1 FIXED-FIXED BERNOULLI-EULER BEAM

The first example is a simple fixed-fixed Bernoulli-Euler beam shown in Fig. 4. The beam has elastic modulus E, second moment of inertia I, density ρ, and cross-sectional area A. Two forces act on the beam at points l_1 and l_2. For this example only two modes are retained resulting in the bond graph of Fig. 5.

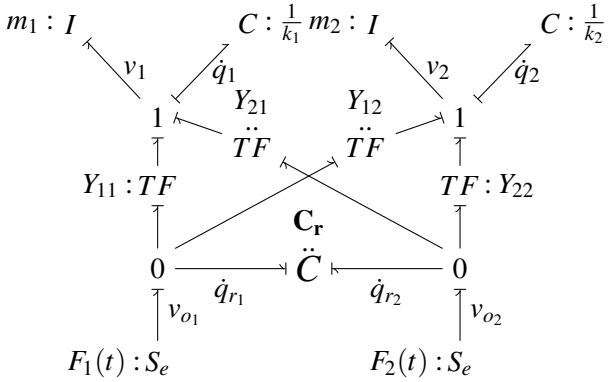

Figure 5: EXAMPLE 1 - FIXED-FIXED BERNOULLI EULER BEAM BOND GRAPH WITH 2 RETAINED MODES

The equations of motion for this system are

$$\dot{p}_1 = -k_1 q_1 + Y_{11}F_1 + Y_{21}F_2 \tag{25}$$

$$\dot{q}_1 = \frac{1}{m_1}p_1 \tag{26}$$

$$\dot{p}_2 = -k_2 q_2 + Y_{12}F_1 + Y_{22}F_2 \tag{27}$$

$$\dot{q}_2 = \frac{1}{m_2}p_2 \tag{28}$$

and the outputs of interest are

$$v_{o_1} = \frac{Y_{11}}{m_1}p_1 + \frac{Y_{12}}{m_2}p_2 + c_{r_{11}}\dot{F}_1 + c_{r_{12}}\dot{F}_2 \tag{29}$$

$$v_{o_2} = \frac{Y_{21}}{m_1}p_1 + \frac{Y_{22}}{m_2}p_2 + c_{r_{21}}\dot{F}_1 + c_{r_{22}}\dot{F}_2 \tag{30}$$

The fixed-fixed beam has the same frequency equation as the free-free solution or

$$\cosh k_n L \cos k_n L = 1 \tag{31}$$

In order to calculate the residual compliances for the fixed-fixed beam shown above, the equation is needed for the deflection of a beam under a point load. For beam with a single point load applied at $x = a$, as shown in Fig. 6, the deflection at any point on the beam can be found with the Eq. (32) and (33) (Box 2004).

$$\delta(x \le a) = F\frac{x^2(L-a)^2(3aL - xL - 2xa)}{6EIL^3} \tag{32}$$

$$\delta(x > a) = F\frac{x^2(L-a)^2(3aL - xL - 2xa)}{6EIL^3} + F\frac{(x-a)^3L^3}{6EIL^3} \tag{33}$$

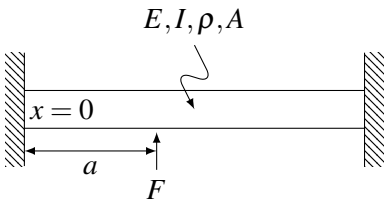

6

Figure 6: EXAMPLE 1 - FIXED-FIXED BERNOULLI EULER BEAM

Now for a fixed-fixed beam with multiple forces, the deflection at each point can be found by the principle of superposition (Bedford, Fowler, and Liechti 2003). The total deflections at l_1 and l_2 for the system of Fig. 4 are found to be

$$\delta(l_1) = \frac{l_1^3(L-l_1)^3}{3EIL^3}F_1 + \frac{l_1^2(L-l_2)^2(3l_2L-l_1L-2l_1l_2)}{6EIL^3}F_2 \quad (34)$$

$$\delta(l_2) = \frac{l_1^2(L-l_2)^2(3l_2L-l_1L-2l_1l_2)}{6EIL^3}F_1 + \frac{l_2^3(L-l_2)^3}{3EIL^3}F_2 \quad (35)$$

This enables the calculation of the residual compliances and can be found using the following equations

$$c_{r_{11}} = \frac{l_1^3(L-l_1)^3}{3EIL^3} - \frac{Y_{11}^2}{k_1} - \frac{Y_{12}^2}{k_2} \quad (36)$$

$$c_{r_{22}} = \frac{l_2^3(L-l_2)^3}{3EIL^3} - \frac{Y_{21}^2}{k_1} - \frac{Y_{22}^2}{k_2} \quad (37)$$

$$c_{r_{12}} = \frac{l_1^2(L-l_2)^2(3l_2L-l_1L-2l_1l_2)}{6EIL^3} - \frac{Y_{11}Y_{12}}{k_1} - \frac{Y_{12}Y_{22}}{k_2} \quad (38)$$

3.1.1 RESULTS

Start with finding the steady-state values finding steady state results for Eqs. (25-28). This results

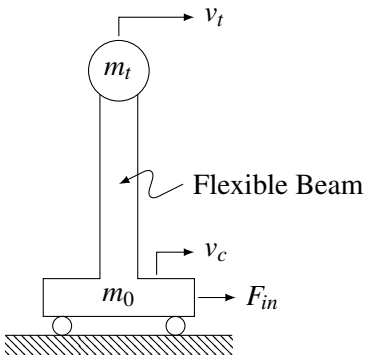

Figure 7: EXAMPLE 2 - FLEXIBLE BEAM CART WITH ATTACHED MASS

in the steady-state values

$$p_{1,ss} = 0 \quad (39)$$

$$q_{1,ss} = \frac{Y_{11}}{k_1}F_1 + \frac{Y_{21}}{k_1}F_2 \quad (40)$$

$$p_{2,ss} = 0 \quad (41)$$

$$q_{2,ss} = \frac{Y_{12}}{k_2}F_1 + \frac{Y_{22}}{k_2}F_2 \quad (42)$$

Now integrating Eqs. (29) and (30) results in the following displacement equations

$$\delta_{ss}(l_1) = Y_{11}q_{1,ss} + Y_{12}q_{2,ss} + c_{r_{11}}F_1 + c_{r_{12}}F_2 \quad (43)$$

$$\delta_{ss}(l_2) = Y_{21}q_{1,ss} + Y_{22}q_{2,ss} + c_{r_{21}}F_1 + c_{r_{22}}F_2 \quad (44)$$

Now substituting $q_{1,ss}$, $q_{2,ss}$, $c_{r_{11}}$, $c_{r_{12}}$, $c_{r_{21}}$, and $c_{r_{22}}$ into the above equations will result in the deflections of Eqs. (34) and (35). Doing the algebra is left as an exercise for the interested reader.

CART WITH A MASS ATTACHED TO A FLEXIBLE BEAM

In this simple example, shown in Fig. 7, a with a mass attached to the tip of a flexible beam is analyzed. From FEA simulations it is known that only the first non-rigid mode needs to be retained. Using this knowledge, the complete bond graph can be seen in Fig. 8.

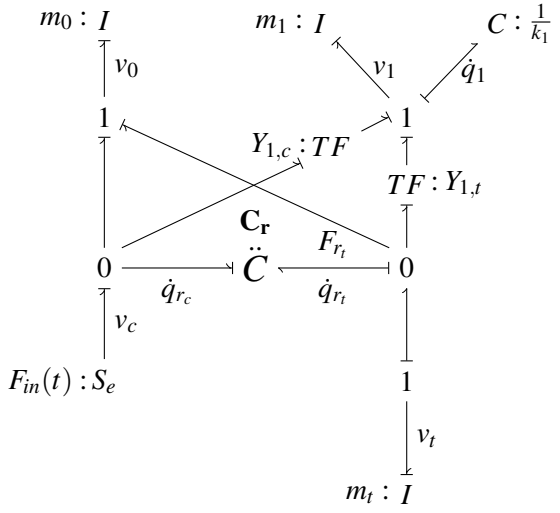

Figure 8: EXAMPLE 2 - BOND GRAPH

3.1.2 SOLVING THE DERIVATIVE CAUSALITY

To solve with the derivative causality on the compliance field, insert the following values into Eq. (22).

$$\mathbf{F_o} = F_{r_t} \tag{45}$$
$$\mathbf{F_i} = F_{in} \tag{46}$$
$$\mathbf{q_o} = q_{r_c} \tag{47}$$
$$\mathbf{q_i} = q_{r_t} \tag{48}$$
$$\mathbf{C_{ii}} = c_{r_{21}} \tag{49}$$
$$\mathbf{C_{io}} = c_{r_{22}} \tag{50}$$
$$\mathbf{C_{oi}} = c_{r_{11}} \tag{51}$$
$$\mathbf{C_{oo}} = c_{r_{12}} \tag{52}$$

Where q_{r_c} and q_{r_t} are the residual steady-state deflections that result from the application of forces at the base and tip. In our case, $F_1 \triangleq F_{in}$ and $F_2 \triangleq F_{r_t}$ is the force resulting from the displacement across the residual compliance. c_{ij} are calculated using Eq. (17). This results in the following system of equations

$$\begin{bmatrix} F_2 \\ q_{r_c} \end{bmatrix} = \begin{bmatrix} -c_{r_{21}}/c_{r_{22}} & 1/c_{r_{22}} \\ c_{r_{11}} - c_{r_{12}}c_{r_{21}}/c_{r_{22}} & c_{r_{12}}/c_{r_{22}} \end{bmatrix} \begin{bmatrix} F_1 \\ q_{r_t} \end{bmatrix} \tag{53}$$

Using this relationship, the equations of motion can be generated using standard bond graph equation formulation techniques. The resulting equations governing the dynamics of this system are

$$\dot{p}_0 = \frac{1}{c_{r_{22}}} q_{r_t} + \left(1 - \frac{c_{r_{21}}}{c_{r_{22}}}\right) F_{in} \tag{54}$$
$$\dot{p}_1 = -k_1 q_1 + \frac{Y_{1,t}}{c_{r_{22}}} q_{r_t} + \left(Y_{1,c} - \frac{Y_{1,t} c_{r_{21}}}{c_{r_{22}}}\right) F_{in} \tag{55}$$
$$\dot{q}_1 = \frac{1}{m_1} p_1 \tag{56}$$
$$\dot{q}_{r_t} = \frac{1}{m_t} p_t - \frac{1}{m_0} p_0 - \frac{Y_{1,t}}{m_1} p_1 \tag{57}$$
$$\dot{p}_t = -\frac{1}{c_{r_{22}}} q_{r_t} + \frac{c_{r_{21}}}{c_{r_{22}}} F_{in} \tag{58}$$

The derivative causality on the residual compliance results in the input force fed through to the tip location while the acausal bond on the residual compliance is not utilized during equation formulation. However, it will be used to derive any of the flow outputs attached to the left 0-junction. For this example, a logical output to monitor would be the differential velocity and position between the cart base and tip mass, $v_c - v_t$ and $\int (v_c - v_t) dt$ respectively. These outputs are found with the following equations

$$v_t = \frac{1}{m_t} p_t \tag{59}$$
$$v_c = \frac{1}{m_0}\left(1 - \frac{c_{r_{12}}}{c_{r_{22}}}\right) p_0 + \frac{1}{m_1}\left(Y_{1,c} - \frac{c_{r_{12}} Y_{1,t}}{c_{r_{22}}}\right) p_1 + \frac{c_{r_{12}}}{c_{r_{22}} m_t} p_t + \left(c_{r_{11}} - \frac{c_{r_{12}} c_{r_{21}}}{c_{r_{22}}}\right) \dot{F}_{in} \tag{60}$$

3.1.3 RESULTS

The system was built in Siemens NX Motion (Seimens 2021) and simulated without the tip mass. The results were then analyzed using IMAT (Engineering 2021) to extract the modes, mode shapes, and modal compliances of a cart with a mass of 0.104 kg. IMAT outputs mass normalized values so $m_j = 1$ kg $\forall\ j$. The values for the simulation and outputs from IMAT are shown in Table 1. Using these values and Eq. (17), the residual compliances were calculated and are shown in Fig. 9.

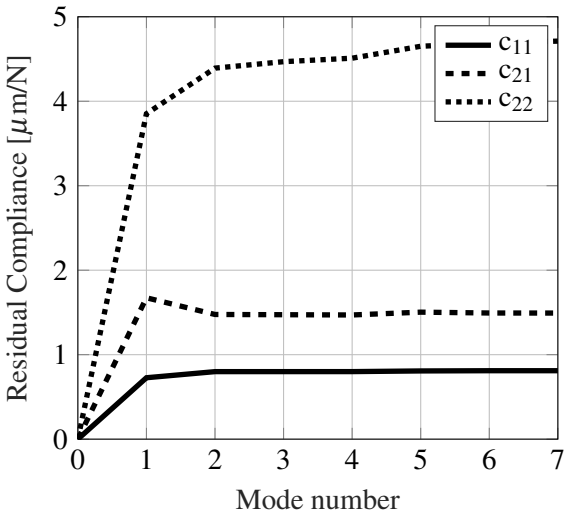

Figure 9: EXAMPLE 2 - RESIDUAL COMPLIANCES VS CONSIDERED MODES

It should be clear that The compliances converge quickly as additional modes are considered.

Table 1: Modal Parameters

mode	f [Hz]	$Y_{i,c}$	$Y_{i,t}$	C$\times 10^{-5}$ [m/N]
1	94	2.95	-6.66	0.2858
2	515	-2.76	-6.35	0.0095
3	1195	-2.02	5.52	0.0018
4	1669	0.15	-2.90	0.0009
5	1669	-0.11	2.13	0.0009
6	2482	1.38	5.86	0.0004
7	3760	1.23	-4.54	0.0002
8	4489	0.14	-4.34	0.0001

After convergence, the residual compliances are found to be

$$c_{r_{11}} = 8.10 \times 10^{-7} \tag{61}$$

$$c_{r_{21}} = c_{r_{12}} = 1.49 \times 10^{-6} \tag{62}$$

$$c_{r_{22}} = 4.71 \times 10^{-6} \tag{63}$$

Using the residual compliance values and the information for the first mode in Table 1, the state space system is

$$\dot{p}_0 = 212240 q_{r_t} + 0.6832 F_{in} \tag{64}$$

$$\dot{p}_1 = -349860 q_1 - 1143800 q_{r_t} + 5.0552 F_{in} \tag{65}$$

$$\dot{q}_1 = p_1 \tag{66}$$

$$\dot{q}_{r_t} = -9.6167 p_0 + 6.6611 p_1 + \frac{1}{m_t} p_t \tag{67}$$

$$\dot{p}_t = -212240 q_{r_t} + 0.3168 F_{in} \tag{68}$$

Using these equations, the determinate of the system can be parameterized by m_t

$$\begin{aligned} \det A = s^4 + (100.1 + \frac{2.1}{m_t}) \times 10^5 s^2 \\ + (71.41 + \frac{7.42}{m_t}) \times 10^{10} \end{aligned} \tag{69}$$

This shows that including the residual compliance adds an additional mode that estimates the effects of residual compliance in the system due to pruned modes. Using this equation, one can easily analyze the effects that the tip mass has on this system. This shows how the resonance frequencies change

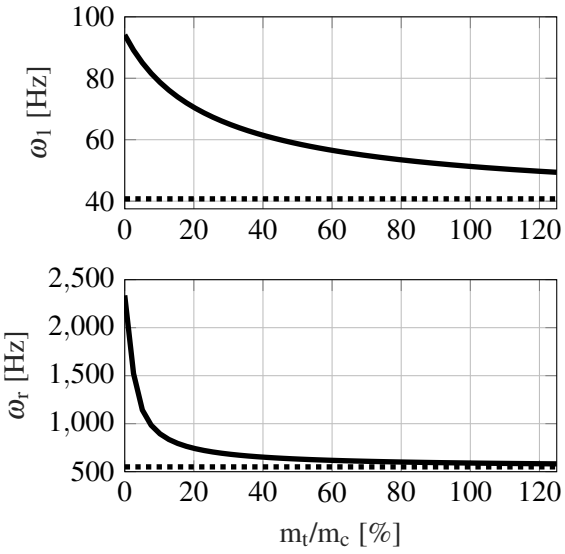

Figure 10: EXAMPLE 2 - NATURAL FREQUENCIES AS TIP MASS CHANGES

as the tip mass increases. The higher (residual) mode converges much faster while the lower (included) mode does not converge as quickly. The two modes converge to 40.75 and 550 Hz respectively. For many analyses and control designs,

these frequencies may be much faster than are required but may affect the performance depending on what the requirements are. Further, without the residual compliance, the residual mode would not be apparent in this system. This is an additional advantage when including residual compliances in the system. It will allow for higher order dynamics due to system level interactions to be analyzed.

CONCLUSIONS

In this paper a method of including residual compliances in finite mode representations of continuous structural elements was developed. Including this residual compliances allows, not just correct steady-state deflections, but inclusion of relevant residual system level modes that occur when modal models are interconnected. Further, residual compliances can assist in correcting acausal bond graphs. Two examples were shown for a basic fixed-fixed Bernoulli-Euler beam as well as the effects on a cart with a mass attached to a flexible beam. These examples showed the validity of the method as well as its usefulness in integrating finite mode models into more complex systems.

REFERENCES

Bedford, A., W. L. Fowler, and K. M. Liechti. 2003. *Statics and mechanics of materials*. Prentice Hall/Pearson Education.

Blelloch, P. A., J. Dickens, A. Majed, and J. Sills. 2019. "Application of Modal Truncation Vectors to the Mixed and Fixed Boundary Dynamic Math Models". In *AIAA Scitech 2019 Forum*, pp. 0495.

The Engineering Tool Box 2004. "Beams - Fixed at Both Ends - Continuous and Point Loads".

ATA Engineering 2021. "IMAT".

Karnopp, D. C., D. L. Margolis, and R. C. Rosenberg. 2012. *System dynamics: modeling, simulation, and control of mechatronic systems*. John Wiley & Sons.

Margolis, D. L. 1985. "A survey of bond graph modelling for interacting lumped and distributed systems". *Journal of the Franklin Institute* vol. 319 (1-2), pp. 125–135.

Mukherjee, R., N. Siegler, and H. Thronson. 2019. "The future of space astronomy will be built: results from the in-space astronomical telescope (iSAT) assembly design study". In *70th International Astronautical Congress (IAC)*, pp. 21–25.

Petersen, K. B., M. S. Pedersen et al. 2008. "The matrix cookbook". *Technical University of Denmark* vol. 7 (15), pp. 510.

Seimens 2021. "NX Motion".

AUTHOR BIOGRAPHIES

LAYNE CLEMEN is the Director of Building Technologies at Extensible Energy in California. He has held positions working in mechatronic product development, aerospace and defense applications of modeling and control, and most recently development of predictive energy management and demand response for commercial buildings. His email is layne@extensibleenergy.com.

DONALD L. MARGOLIS is Professor of Mechanical Engineering Co-Director of the Hyundai Center for Excellence at UC Davis. He has extensive experience in teaching system dynamics at the graduate and undergraduate levels, consultation in the vibration control industry, and has published numerous papers on the industrial applications of the dynamics. His email is dlmargolis@ucdavis.edu.